Dielectrophoretic spectra of translational velocity and critical frequency for a spheroid in traveling electric field

Sakshin Bunthawin,[1,2,a)] Pikul Wanichapichart,[2,3] Adisorn Tuantranont,[4] and Hans G. L. Coster[5]
[1]*Biotechnology of Electromechanics Research Unit, Faculty of Technology and Environment, Prince of Songkla University, Phuket 83120, Thailand*
[2]*Department of Physics, Membrane Science and Technology Research Center, Prince of Songkla University, Hatyai 90110, Thailand*
[3]*NANOTEC Center of Excellence, Prince of Songkla University, Hatyai 90110, Thailand*
[4]*Nano-Electronics and MEMs Laboratory, National Electronics and Computer Technology Center, Pathumthani 12120, Thailand*
[5]*School of Chemical and Biomolecular Engineering, University of Sydney, New South Wales 2006, Australia*

(Received 16 October 2009; accepted 22 December 2009; published online 13 January 2010)

An analysis has been made of the dielectrophoretic (DEP) forces acting on a spheroidal particle in a traveling alternating electric field. The traveling field can be generated by application of alternating current signals to an octapair electrode array arranged in phase quadrature sequence. The frequency dependent force can be resolved into two orthogonal forces that are determined by the real and the imaginary parts of the Clausius–Mossotti factor. The former is determined by the gradient in the electric field and directs the particle either toward or away from the tip of the electrodes in the electrode array. The force determined by the imaginary component is in a direction along the track of the octapair interdigitated electrode array. The DEP forces are related to the dielectric properties of the particle. Experiments were conducted to determine the DEP forces in such an electrode arrangement using yeast cells (*Saccharomyces cervisiate* TISTR 5088) with media of various conductivities. Experimental data are presented for both viable and nonviable cells. The dielectric properties so obtained were similar to those previously reported in literature using other DEP techniques. © *2010 American Institute of Physics.* [doi:10.1063/1.3294082]

I. INTRODUCTION

Traveling wave dielectrophoresis (twDEP) is being investigated as a possible tool for medical diagnostics, drug delivery, and cell therapeutics based on selection, isolation, concentration, purification, and separation of bioparticle mixtures.[1,2] The fields employed for such work are generated using electrodes such as planar linear interdigitated arrays[3,4,1] or two parallel arrays.[5–7,2,8] The electrodes in these arrays are driven by sinusoidal quadrature-phase voltages. The phase sequence addressing employed has been described by many investigators.[5,7,3,4,1,8] The two parallel electrode arrays offer advantages for cell manipulation and positioning. The methods allow cells to move either toward the electrode tips or along the electrode track simultaneously as a result of two orthogonal forces. Wang *et al.*[7] termed them the "unified force" which depends on the real Clausius–Mossotti factor (Re[CMF]) and the imaginary part (Im[CMF]) of the complex dielectric-frequency dependent CMF. The polarity of Re[CMF] and Im[CMF] calculated from the unified force (whether they are positive, negative, or zero) indicates the direction of cell movement in the traveling electric field.

[a)]Electronic mail: sakshin@phuket.psu.ac.th.

In the past, the positive conventional dielectrophoretic (cDEP) force and Re[CMF] were employed to estimate cell dielectric properties through microscopic measurements of cell translational and cell spin velocities.[9,10] However measurements using such a technique at lower frequencies are difficult to make and the technique does not lend itself to measuring negative DEP forces. This limits the ability to accurately determine the dielectric properties of cell membranes by this technique. To overcome this problem, another approach was introduced by Gimsa and Wachner[11] based on an RC model of the cell. Using that model the two critical frequencies at the crossover points between positive and negative functions of Re[CMF] at lower (f_ℓ) and higher (f_h) frequency can be used to determine the cell parameters. This model was later extended by Bunthawin and Wanichapichart.[12]

Here we present an extension of the "unified" force proposed by Wang *et al.*[7] to spheroidal cells because many cells of interest are spheroidal rather than simple spheres. We also present experimental measurements of cell velocities for positive dielectrophoresis (but not twDEP) and these are compared with the extended theoretical model.

II. THEORETICAL APPROACH

A. The traveling dielectrophoretic force

The time-average DEP force ($\bar{\vec{F}}_t$) acting on a dielectric particle in a nonuniform sinusoidal electric field $\vec{E}_k(t)$ is given by (see Wang *et al.*[7])

$$\bar{\vec{F}}_t = \sum_{k=x,y,z} \left(\mu_{\mathrm{eff}(x)}(t)\frac{\partial E_k(t)}{\partial x} + \mu_{\mathrm{eff}(y)}(t)\frac{\partial E_k(t)}{\partial y} + \mu_{\mathrm{eff}(z)}(t)\frac{\partial E_k(t)}{\partial z} \right)\hat{a}_k \tag{1}$$

where $\hat{a}_k(k=x,y,z)$ are unit vectors in the Cartesian coordinate frame, $\vec{E}_k(t) = \Sigma_{k=x,y,z} E_k \cos(\omega t + \phi_k)\hat{a}_k$, and the effective dipole moment $\vec{\mu}_{\mathrm{eff}(k)}$ for a spheroid possessing the volume $\frac{4}{3}\pi ab^2$ [Figs. 1(a) and 1(b)] can be expressed as

$$\vec{\mu}_{\mathrm{eff}(k)}(t) = \sum_{k=x,y,z} \frac{4}{3}\pi ab^2 \varepsilon_0 \varepsilon_s E_k(t)(\cos(\omega t + \phi_k)\mathrm{Re[CMF]} - \sin(\omega t + \phi_k)\mathrm{Im[CMF]})\hat{a}_k. \tag{2}$$

Substituting Eq. (2) into Eq. (1) gives

$$\bar{\vec{F}}_t = \sum_{k=x,y,z} \frac{4}{3}\pi ab^2 \varepsilon_0 \varepsilon_s \left(\mathrm{Re[CMF]}\frac{\partial(E_x^2 + E_y^2 + E_z^2)}{2\,\partial k} + \mathrm{Im[CMF]}\left(E_x^2\frac{\partial \phi_x}{\partial k} + E_y^2\frac{\partial \phi_y}{\partial k} + E_z^2\frac{\partial \phi_z}{\partial k} \right) \right)\hat{a}_k. \tag{3}$$

Rearranging Eq. (3) using the gradient operator yields

$$\bar{\vec{F}}_t = \tfrac{2}{3}\pi ab^2 \varepsilon_0 \varepsilon_s [\mathrm{Re[CMF]}\,\nabla E^2 + \mathrm{Im[CMF]}(E_x^2\,\nabla\,\phi_x + E_y^2\,\nabla\,\phi_y + E_z^2\,\nabla\,\phi_z)], \tag{4}$$

where E is the root mean square (rms) value of the electric field strength. The time-average DEP force ($\bar{\vec{F}}_t$) of the spheroid can be resolved into the cDEP force ($\vec{F}_{\mathrm{cDEP}}$) and traveling wave DEP force ($\vec{F}_{\mathrm{twDEP}}$). The former attracts the spheroid to the tip of the electrode and the latter pushes it along the track (see Fig. 2). As can be seen from Eq. (4), the first term is related to the cDEP force as proposed previously by Pohl[13] and Jones.[4] The magnitude of the $\vec{F}_{\mathrm{cDEP}}$ depends on both Re[CMF] and ∇E^2 while the force direction depends on whether Re[CMF]>0 or Re[CMF]<0. For twDEP, the Im[CMF] and $\nabla\phi_k$ influence the magnitude and direction of the $\vec{F}_{\mathrm{twDEP}}$, respectively. The factor $\nabla\phi_k$ indicates that the force due to the traveling electric field is in the direction of the gradient in the phase, that is, the force directs the cell toward the regions where the phase of the field component is larger (for Im[CMF]>0) or smaller (for Im[CMF]<0). It is interesting that both forces ($\vec{F}_{\mathrm{cDEP}}$ and $\vec{F}_{\mathrm{twDEP}}$) are not synchronized and usually predominate at different electric field frequencies.

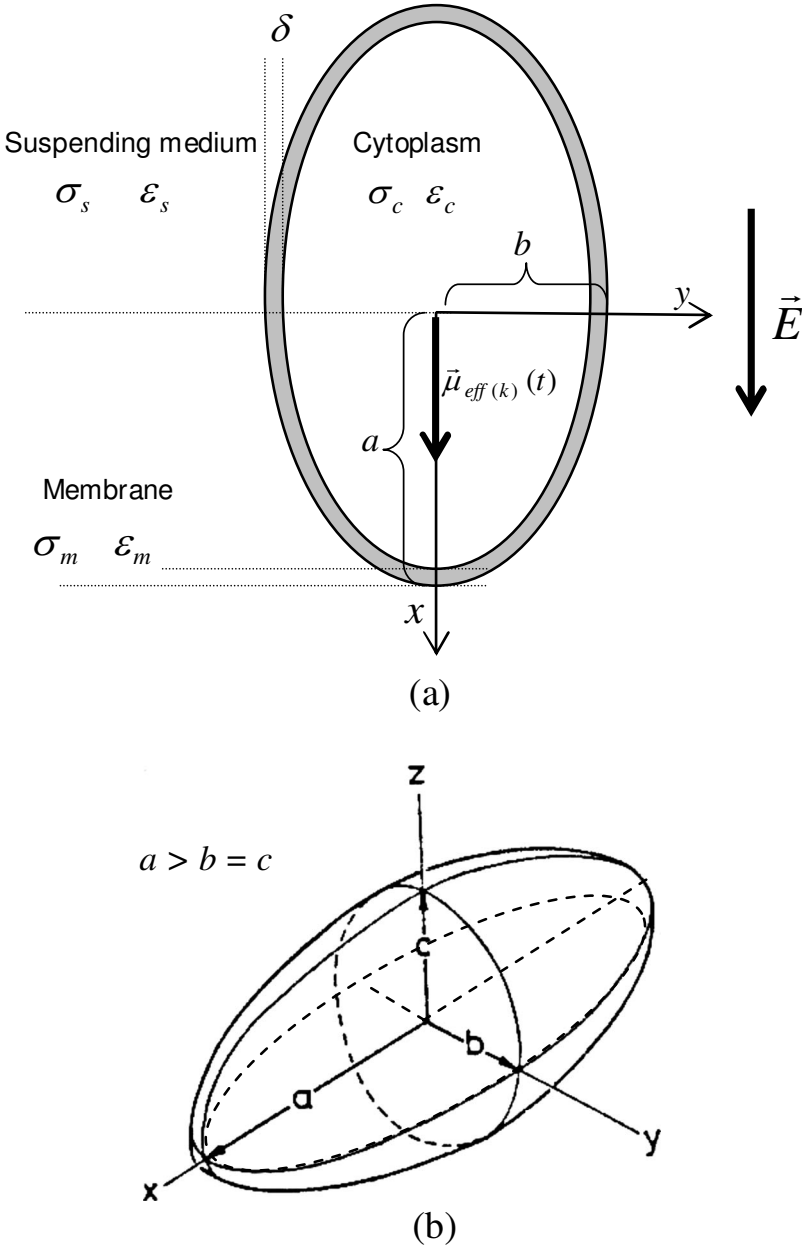

FIG. 1. A single shelled spheroidal model in ac electric field ($\vec{E}$) related with the effective dipole moment vector $\vec{\mu}_{\text{eff}(k)}$. (a) Cross sectional view of the shelled spheroid assigned with dielectric constants and conductivities of the suspending medium (ε_s, σ_s), the cytoplasm (ε_c, σ_c), and the membrane (ε_m, σ_m). (b) Three dimensional view showing three a, b, and c axes along x, y, and z, respectively. The δ is denoted for the membrane thickness.

It should be noted that electric field strength (E) and its components (E_x, E_y, E_z) originating from an interdigitated electrode can be simulated through the finite elements analysis program QUICK FIELD™ version 5.5. This field analysis program was used to map the field strength using the phase sequence and electrode geometry described in Fig. 2. This procedure provided numerical values of the electric field strengths between the electrodes with the maximum values located at the tips. Differentiation of the electric field strengths between two very closely spaced points then allowed us to obtain accurate values of the electric field gradient (∇E^2). These calculations were performed using signals of 0.7, 1.4, 2.8, and 7.0 V (rms) applied to the electrodes and these

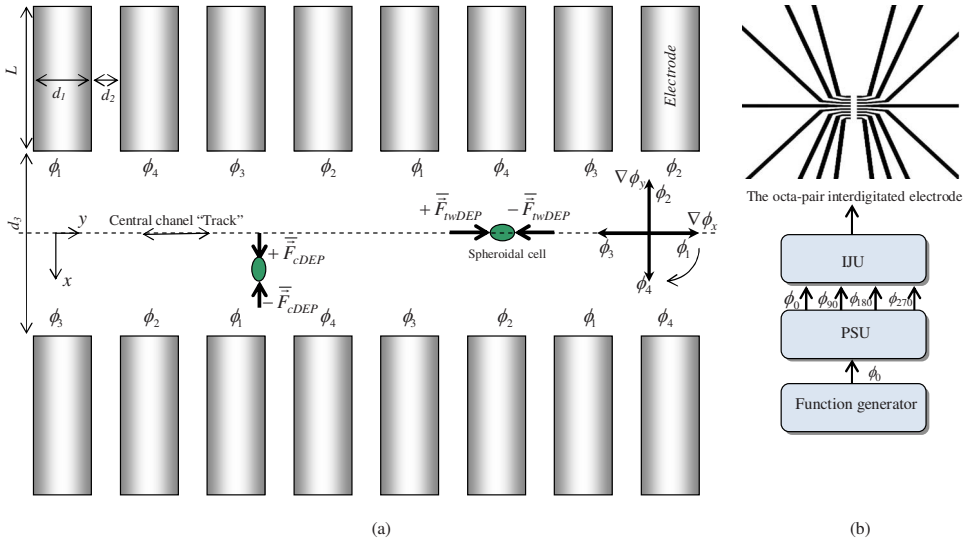

FIG. 2. The top view of the octapair interdigitated electrode with diagrams of electrical setup to operate the electrode. (a) Two orthogonal forces ($\bar{\bar{F}}_{\mathrm{cDEP}}$ and $\bar{\bar{F}}_{\mathrm{twDEP}}$) acting on the spheroid in $\pm x$ and $\pm y$ directions, respectively. (b) The electrode was driven by the quadrature phase signals split from a function generator through the interjunction unit connected with phase shift unit.

correspond to maximum field strengths of 14, 28, 57, and 143 kV m^{-1}, respectively.

B. The Clausius–Mossotti factor of the spheroid

Consider a spheroidal model composed of two compartments with different dielectric properties, as shown in Fig. 1(a). The effective value of the complex relative permittivity of the whole spheroid ($\varepsilon^*_{\mathrm{eff}}$) can be then written[14] as

$$\varepsilon^*_{\mathrm{eff}} = \varepsilon^*_m + \upsilon\left[\frac{1}{(\varepsilon^*_c - \varepsilon^*_m)} + (1-\upsilon)\frac{L_k}{\varepsilon^*_m}\right]^{-1}, \tag{5}$$

where all complex parameters are defined as $\varepsilon^*_i = \varepsilon_i - j\sigma_i(\omega\varepsilon_0)^{-1}$, the fractional volume $\upsilon = (1-\delta/a)(1-\delta/b)^2$, and the depolarization factor (L_k) in either x or y or z axis is given by

$$L_k = -\frac{1}{q^2-1} + \frac{q}{(q^2-1)^{3/2}}\ell n[q + (q^2-1)^{1/2}], \tag{6}$$

where $q = a/b > 1$. The following relationships between the L_k for the three axes hold: $\Sigma_{k=x,y,z}L_k = 1$ and $L_y = L_z = 1 - L_x/2$. We define here also a complex-frequency dependent CMF (see Ref. 15),

$$[\mathrm{CMF}] = \frac{\varepsilon^*_{\mathrm{eff}} - \varepsilon^*_s}{\varepsilon^*_s + (\varepsilon^*_{\mathrm{eff}} - \varepsilon^*_s)L_k}. \tag{7}$$

Substituting Eqs. (5) and (6) into Eq. (7) yields the explicit expression of the CMF. The real and the imaginary parts of the CMF are

$$\mathrm{Re}[\mathrm{CMF}] = \left[\left(\frac{Z_1Z_3 + Z_2Z_4}{Z_3^2 + Z_4^2}\right)\right], \tag{8}$$

$$\mathrm{Im[CMF]} = \left[\left(\frac{Z_1 Z_3 - Z_2 Z_4}{Z_3^2 + Z_4^2}\right)\right], \tag{9}$$

where

$$Z_1 = \mathrm{Re}[\varepsilon_{\mathrm{eff}}^*] - \omega\varepsilon_0\varepsilon_s,$$

$$Z_2 = \mathrm{Im}[\varepsilon_{\mathrm{eff}}^*] - \sigma_s,$$

$$Z_3 = \omega\varepsilon_0\varepsilon_s(1 - L_k) + \mathrm{Re}[\varepsilon_{\mathrm{eff}}^*]L_k,$$

$$Z_4 = \mathrm{Im}[\varepsilon_{\mathrm{eff}}^*]L_k - \sigma_s(L_k + 1),$$

$$\mathrm{Re}[\varepsilon_{\mathrm{eff}}^*] = \frac{1}{\omega\varepsilon_0}\left(\frac{(\omega^2\varepsilon_0^2\varepsilon_m Z_5 + \sigma_m Z_6)(\omega\varepsilon_0 Z_7) + \omega\varepsilon_0 Z_8(\varepsilon_m Z_6 - \sigma_m Z_5)}{(\omega\varepsilon_0 Z_7)^2 + Z_8^2}\right),$$

$$\mathrm{Im}[\varepsilon_{\mathrm{eff}}^*] = \frac{1}{\omega\varepsilon_0}\left(\frac{\omega^2\varepsilon_0^2 Z_7(\varepsilon_m Z_6 - \sigma_m Z_5) - Z_8(\omega^2\varepsilon_0^2\varepsilon_m Z_5 + \sigma_m Z_6)}{(\omega\varepsilon_0 Z_7)^2 + Z_8^2}\right),$$

and

$$Z_5 = \varepsilon_m + \alpha(\varepsilon_c - \varepsilon_m),$$

$$Z_6 = \alpha(\sigma_m - \sigma_c) - \sigma_m,$$

$$Z_7 = \varepsilon_m + \beta(\varepsilon_c - \varepsilon_m),$$

$$Z_8 = \beta(\sigma_m - \sigma_c) - \sigma_m,$$

where $\alpha = L_k + v(1 - L_k)$ and $\beta = L_k(1 - v)$.

The first and the second terms in the bracket of Eq. (4) refer to Eqs. (8) and (9), respectively. For a spheroid, the Re[CMF], as mentioned in Eq. (8), is affected by the dielectric and conductivity parameters of the cytoplasm $(\varepsilon_c, \sigma_c)$, the membrane $(\varepsilon_m, \sigma_m)$, and the suspending medium $(\varepsilon_s, \sigma_s)$. The theoretical spectra of Re[CMF] for various dielectric properties of the system are shown in Fig. 3. The values of the parameters chosen were of particular relevance to yeast cells, and for these calculations the thickness of cell membrane, including the cell wall, was assumed to be 12 nm.

A striking feature of the theoretical spectra is the prediction that of a sharp peak in the Re[CMF], which determines the magnitude of the DEP velocity, at frequencies close to and immediately following the lower critical frequency (around 200 kHz). Beyond this peak the Re[CMF] relaxes back to a plateau until frequencies approaching the upper critical frequency. This sharp peak is not predicted by the theory based on spherical particle (e.g., see Ref. 9). The peak predicted from the analysis given here for a spheroidal particle is not affected by changes in ε_c and ε_s. For lower positive values of Re[CMF] an increase in ε_m shifted the f_ℓ to the lower values, while the increased σ_c shifts the f_h to the higher frequencies and higher positive force. Increasing values of σ_c increase the peak height of the force. Increasing the conductivity of the membrane (σ_m) from 10^{-7}–10^{-5} S m^{-1} shifts the peak to lower frequencies.

C. Translational velocity

A force diagram of the spheroid (cell) being levitated above the electrode in the viscous medium is shown in Fig. 4. Evaluation of translational speed of the spheroid was made by using

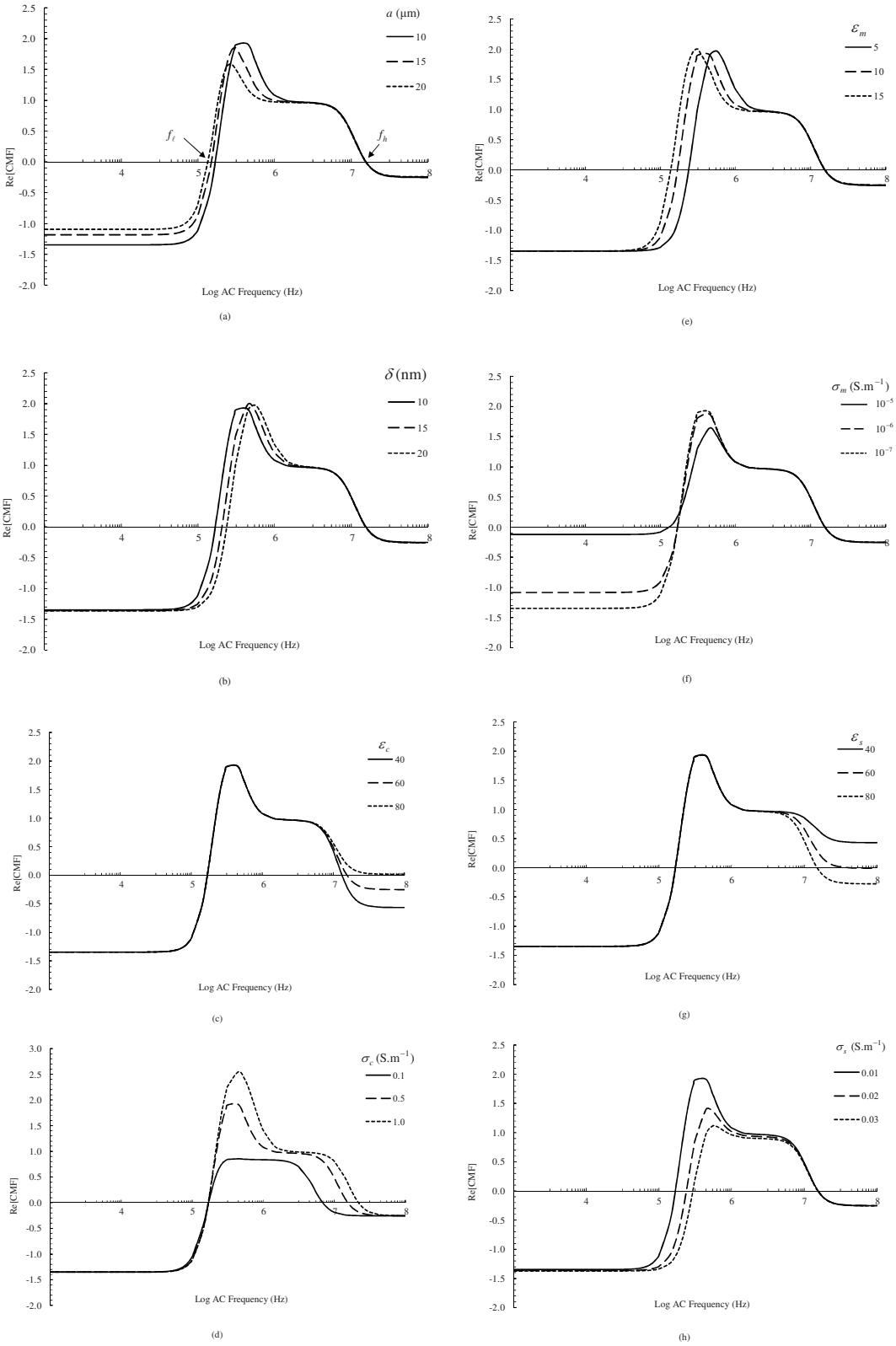

FIG. 3. The spectra of Re[CMF] are affected by changing electrical parameters of the spheroidal model, as described in Fig. 1.

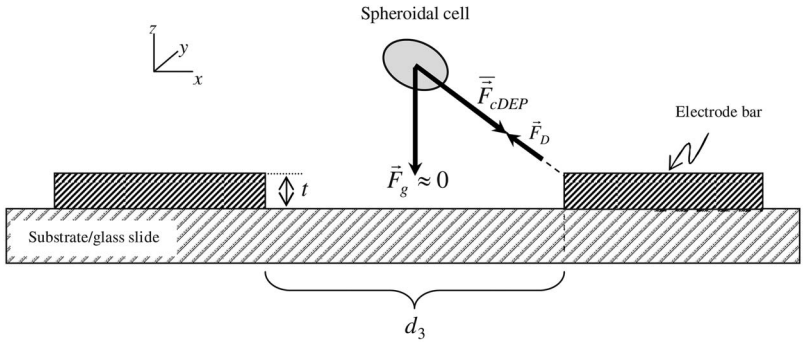

FIG. 4. Cross-sectional view of the interdigitated electrode, as seen from x-z plane (not to scale), shows forces acting on the cell being levitated above the track.

Newton's law of motion. To reduce complicated mathematical analysis, the mass density of the cell (ρ_{cell}) is assumed to be approximately equal to that of the suspending medium (ρ_{medium}), hence, the gravitational force is $\vec{F}_g = (4/3)\pi ab^2(\rho_{\text{cell}} - \rho_{\text{medium}})\vec{g} \approx 0$.

Also, the electric field gradient was assumed to be so low that the translational velocity of the spheroid will be essentially constant, that is, the particle has reached terminal velocity where the translational force is balanced by the frictional drag force. The drag force for the case of a spheroid is now given by Happel and Brenner,[16]

$$\vec{F}_D = 6\pi\eta\vec{v}aK'\hat{a}_k, \tag{10}$$

where η is the viscosity of the suspending medium and K' is a shape factor given by

$$K' = \frac{\frac{4}{3}(\gamma^2 - 1)}{\frac{(2\gamma^2 - 1)}{(\gamma^2 - 1)^{1/2}}\ln[\gamma + (\gamma^2 - 1)^{1/2}] - \gamma}, \quad \gamma = \frac{b}{a}. \tag{11}$$

If Im[CMF]=0 and Re[CMF]$\neq$0, Eq. (4) becomes

$$\vec{\bar{F}}_{\text{cDEP}} = -\vec{F}_D, \tag{12}$$

and Re[CMF]=0 and Im[CMF]$\neq$0, then

$$\vec{\bar{F}}_{\text{twDEP}} = -\vec{F}_D. \tag{13}$$

Substituting the first and the second forces of Eq. (4) into Eqs. (12) and (13) yields the translational speed as

$$\vec{v}_{\text{cDEP}} = \frac{\varepsilon_0\varepsilon_s b^2\,\text{Re}[\text{CMF}]\,\nabla E^2}{9\eta K'}\hat{a}_{\pm x} \tag{14}$$

and

$$\vec{v}_{\text{twDEP}} = \frac{\varepsilon_0\varepsilon_s b^2\,\text{Im}[\text{CMF}]\sum\limits_{i=x,y,z}(E_i^2\nabla\phi_i)}{9\eta K'}\hat{a}_{\pm y}. \tag{15}$$

As is seen from Eqs. (14) and (15), the direction of $\vec{v}_{\text{cDEP}}$ and $\vec{v}_{\text{twDEP}}$ depends on the polarity of the Re[CMF] and Im[CMF], respectively. Both velocities are a function of the dielectric properties and they are frequency dependent. In case of the conventional force, the spheroid will experience positive dielectrophoresis if the field frequency is in the range from f_ℓ to f_h [Eqs. (A1) and (A2)].

III. EXPERIMENTAL

A. Microelectrode fabrication

An octapair interdigitated gold electrode was fabricated on microscope glass slides of dimension $80 \times 30 \times 1$ mm^3 (Marienfeld, Germany). The electrode array was made of gold and was 200 μm in length (L), 100 μm in width (d_1), and 0.2 μm in thickness (t). The separation of the adjacent bars on the same array (d_2) was 100 μm and that for two opposite arrays (microchannel width) was 300 μm (d_3). The track length was about 1500 μm (Fig. 2). Detailed information relating to all process is provided by Fu *et al.*[8]

B. Electrical setup

A synthesized function generator (Stanford Research Systems, Model DS345) was connected to the electrode array, as shown in Fig. 2(b).

C. Cell preparation and data collection

Yeast cells, *Saccharomyces cervisiate* TISTR 5088, were determined as a prolate spheroid of $4.0 \pm 0.7 \times 3.0 \pm 0.4$ μm. They were obtained from the Department of Biotechnology, Faculty of Agro-Industry, Prince of Songkla University. Cells were grown in $70 g \ell^{-1}$ of peptone yeast extract agar (PDA, Criterion) at 27 °C with incubator shaker (Jencons Scientific, model JS201) at 200 rpm.[17] The cells were harvested in the stationary phase after 24 h and washed twice with deionized water, then centrifuged at $1000 \times$ g for 2 min and resuspended twice in 0.5M sorbitol solution. The solution conductivity (σ_s) was measured by using a conductivity meter (Tetracon 325, LF318), and the conductivity was adjusted from 3 to 300 mS m^{-1} by adding 0.1M KCl solution using a micropipette (Nichipet, model 5000DG).

For the DEP measurements 100 ml aliquots of a diluted cell suspension containing 1.15×10^5 cells/ml were pipetted onto the glass slide between the electrodes. The electrodes were energized with four sinusoidal signals (the quadrature phase) of amplitudes 0.7, 1.4, 2.8, and 7.0 V (rms) in phase sequence. To determine the two critical frequencies (f_ℓ and f_h), the frequency of the applied signals was gradually decreased from the upper value of 30 MHz to the lower values (down to 5 kHz).

The videos of cell translation were recorded using a charge coupled device camera (Sony SLV-Japan) connecting to a microcomputer (Acer, Aspire 4310) via the WINFAST PVR™ program. Three cells being in DEP movements were investigated to calculate for $\vec{v}_{\mathrm{cDEP}}$ at a given field frequency through the program. Electric field profiles were simulated using the QUICK FIELD™ program version 5.5 (www.quickfield.com).

For the experiments with dead cells, the cell suspension was heated to 75 °C for 10 min (Ref. 2) and then cooled down to room temperature.[2,18] The suspension was then centrifuged as described for viable cells. Experimental measurements were made of the DEP force (not for twDEP). We found that the DEP velocity and critical frequencies were not affected by changes in the phase sequence. The dielectric parameters for the cells were then obtained by curve fitting to the theoretical model.

D. Data fitting

In order to fit the experimental data to the theoretical expressions, it is necessary to take into account experimental errors. This allows one to deduce the values of the parameters with a quantitative estimate of the best fit. For the $\vec{v}_{\mathrm{cDEP}}$ spectra, the error χ in fitting the data to the theoretical expression can be defined as

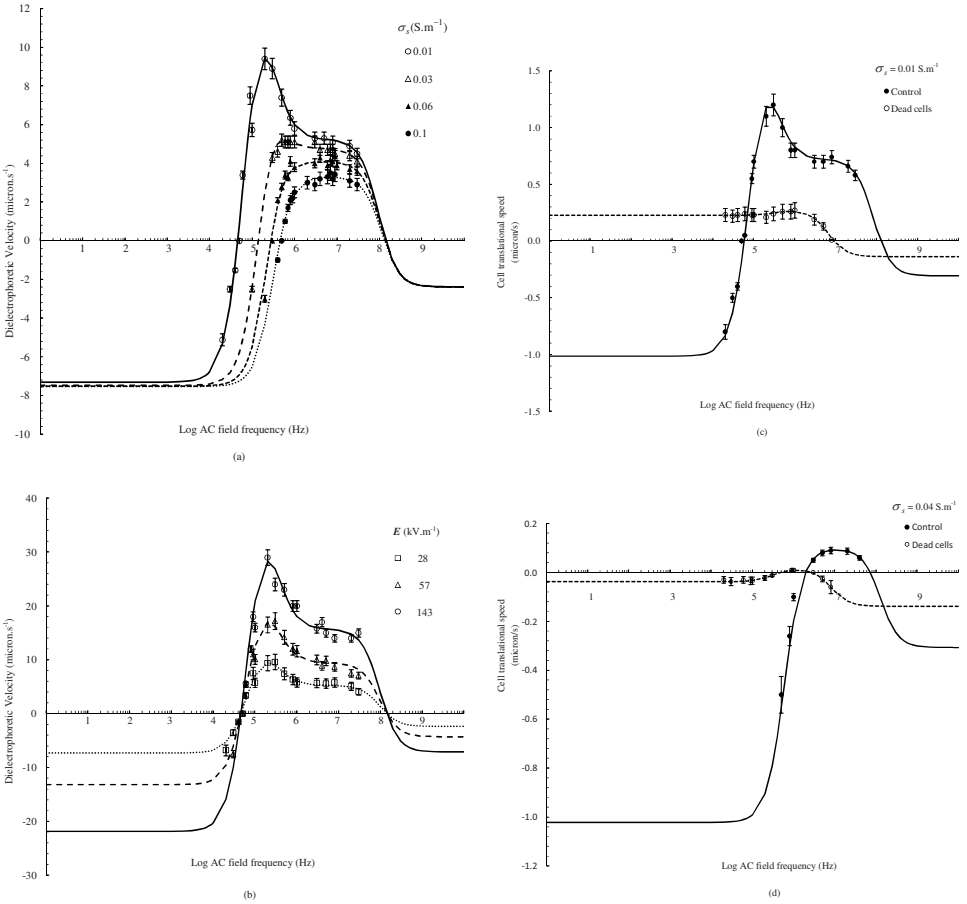

FIG. 5. Curve fittings between experimental and theoretical data of cell translational speeds were plotted as a function of the electric field frequency for the control and dead cells. The conditions are that (a) the conductivities of the suspending medium (σ_s) are changed from 0.01 to 0.10 S m^{-1} and (b) electric field strengths $\boldsymbol{E}$ of 28–143 kV m^{-1}. For the dead cells of $\mathbf{E}$=28 kV m^{-1}, (c) σ_s=0.01 S m^{-1} and (d) σ_s=0.04 S m^{-1}, cells' electrical properties obtained are shown in Table I.

$$\chi = \frac{\sum_{i=1}^{N} \left(\frac{\sqrt{(v_{\text{expt}(i)} - v_{\text{theory}(i)})^2}}{\sqrt{(v_{\text{expt}(i)})^2}} \right)}{N} \times 100, \tag{16}$$

where $v_{\text{expt}(i)}$ and $v_{\text{theory}(i)}$ are the magnitudes of the experimental and the theoretical DEP velocity and N is the number of data points (frequencies). To obtain the best fit it is necessary to minimize Eq. (16) by adjusting the parameters in the theoretical expressions.

The method to fit the theoretical curve with that of the experiments to obtain cell dielectric parameters were made based on the knowledge of sensitivities of dielectric parameters shown in Fig. 3. Theoretical plots in Figs. 5 and 6 showed the fitting results for the DEP velocity spectrum, which gave a value of χ of less than 10%.

IV. RESULTS AND DISCUSSIONS

A. Translational speeds ($\vec{v}_{\text{cDEP}}$) and the lower critical frequency (f_ℓ)

It was observed that the live yeast cells exhibited a positive dielectrophoresis at frequencies from 50 kHz to 30 MHz if the medium conductivity (σ_s) was between 0.01 and 0.30 S m^{-1}. Measurements of cell translational velocity ($\vec{v}_{\text{cDEP}}$) for each experiment provided the data for curve fitting to the theoretical model. Three separate experiments were made for each data plotted

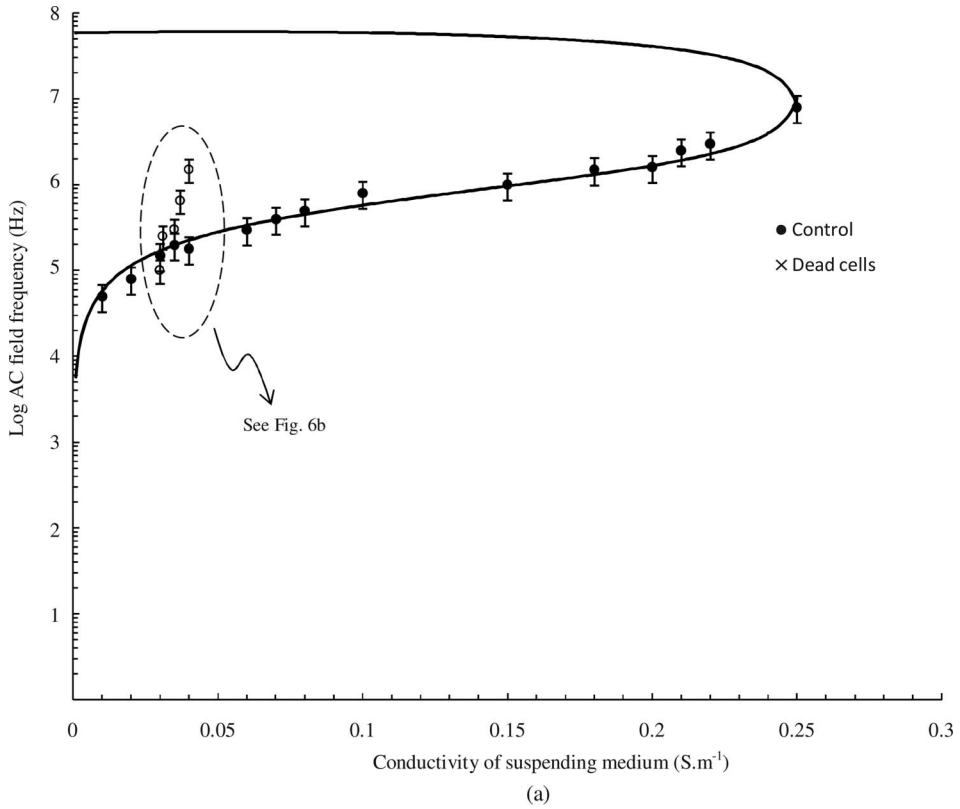

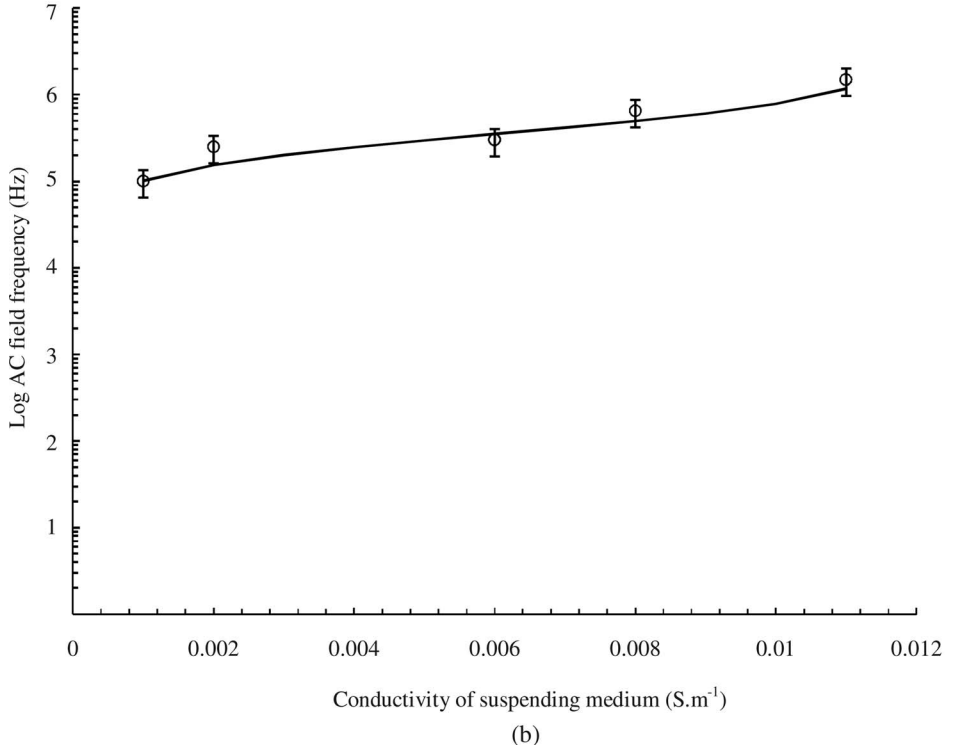

FIG. 6. (a) Curve fittings of critical frequencies of the control and (b) the dead cells as a function of the conductivity of the suspending medium. The theoretical lines were plotted using the parameters shown in Table I.

TABLE I. Summary of the conductivities and dielectric constants of the cytoplasm, the cell membrane, and the suspending medium for the control and dead yeast cells.

Parameters	The control	Dead cells	Living cells[a]
σ_c (S m^{-1})	0.25	0.02	0.20
σ_m (S m^{-1})	1.0×10^{-7}	4.0×10^{-4}	2.5×10^{-7}
ε_c	50	65	50
ε_m	15	25	6
ε_s	78	78	78
a (μm)	4	4	5
$b=c$ (μm)	3	3	4.2
δ (nm)	12	12	8

[a]Reference 19.

in Figs. 5 and 6. The standard deviations that appeared in the DEP velocity (Fig. 5) and the lower critical frequency spectra (Fig. 6), using three replicates, were computed and varied due to experimental measurements. The manual curve fittings of the spectra were performed and the dielectric parameters for the cells so obtained are also tabulated in Table I.

As was expected increasing electric field strengths resulted in increased values of $\vec{v}_{\mathrm{cDEP}}$ and an increase in the peak of the positive spectra. At 28 kV m^{-1}, 300 kHz, and $\sigma_s=0.01$ S m^{-1}, the maximum value of the DEP force was found to be 9.9×10^{-4} pN, which corresponds to $\vec{v}_{\mathrm{cDEP}}=1.2$ μm s^{-1}. Curve fitting of the critical frequencies f_ℓ and f_h of the living and the nonliving cells to the theoretical model are shown in Fig. 6. It should be noted that the electrical properties that were determined from this fitting procedure were essentially the same as that obtained from theoretical fitting to the $\vec{v}_{\mathrm{cDEP}}$ data. The $\vec{v}_{\mathrm{cDEP}}$ method is more suitable for data obtained at an intermediate frequency where the theoretical curves are very sensitive to the values of the conductivity of the cytoplasm (σ_c) and dielectric constant of the membrane (ε_m) [see Figs. 3(d) and 3(e)]. The f_ℓ spectra are highly sensitive to the values of ε_m and σ_m only at the lower frequency.

B. Dielectrophoretic spectra of living and dead cells

From the dielectric and conductance parameters determined by fitting the data to the theoretical model, it is then possible to generate extended theoretical DEP spectra for both the dead cells and the live cells over an extended frequency range, beyond that was measured. Both the real part and the imaginary part appropriate for these cells can so be calculated. This is shown in Fig. 5. The magnitude of the CMF for the living cell (the control) was higher than that of the dead, which infers the conductivity of the cytoplasm (σ_c) of the dead cell was less than that of the living yeast cells (typically, the living cell has a cytoplasmic conductivity of about 0.2 S m^{-1} (Ref. 19).

The values deduced for the electrical parameters of the cells, at least for the living yeast cells, are similar to those published by Zhou *et al.*[19] and Talary *et al.*,[2] except for the value of ε_m. It is not clear whether this value of ε_m obtained in the present study is typical of TISTR 5088 yeast cells in general or that it might indicate the need to extend the spheroid model here presented to a double shell model to account more explicitly for the cell wall. It should be noted that the general appearances of the CMF, both the real and the imaginary spectra [Fig. 5(b)], are the same as reported in the literatures for the living and the dead yeast cells.[2,20]

The specific capacitance (C_m) and conductance (G_m) of the membrane in all cases were also calculated and compared with the parameters, as shown in Table I. From Table I, the results showed that C_m and G_m of the control and dead *S. cervisiate* were 11.06 mF m^{-2}, 8.33 S m^{-2} and 18.44 mF m^{-2}, 33.33×10^3 S m^{-2}, respectively.

V. CONCLUSION

This study derived the cDEP force ($\vec{F}_{\mathrm{cDEP}}$) and the traveling wave DEP force ($\vec{F}_{\mathrm{twDEP}}$) acting on a single-shelled spheroid in an ac electric field. The former depends on the real part of the CMF and electric field gradient while the latter depends on the imaginary part of the CMF and for a traveling electric field the phase difference between adjacent regions. These two forces are directly related to the terminal or "drift" that the cells acquire when suspended in a viscous medium. The measurements of this terminal velocity then allowed the dielectric parameters for the cells to be determined by curve fitting to the theoretical model. Measurements were also made of the lower critical frequency (where the translational DEP force is zero). The velocity-curve fitting method is limited to positive velocity measurements at the lower frequencies while the measurement of the critical frequency at the higher value could not be obtained because our signal generator has a high frequency limit of 30 MHz.

The results from experimentations showed that the living yeast cells (*Saccharomyces cervisiate* TISTR 5088) exhibited positive dielectrophoresis over the frequency ranged from 50 kHz (f_ℓ) to 30 MHz (f_h) if the medium conductivities (σ_s) were between 0.01 and 0.30 S m^{-1}. The value of f_ℓ was shifted toward greater values when σ_s was increased. The spectra of cell translational velocity and critical frequency of the living and dead cells were different and allowed the different dielectric properties of these to be determined. In case the living and dead *S.cervisiae* are mixed with density about 10^5 cells ml^{-1} we cannot differentiate them by tuning the frequency.

ACKNOWLEDGMENTS

This work has been partially supported by the National Nanotechnology Center (NANOTEC), NSTDA, Ministry of Science and Technology, Thailand through its program of Center of Excellence Network. Thanks are also extended to the Department of Biotechnology, Faculty of Agro-Industry for supporting yeast cells and Dr. Raymond Ritchie for help with the manuscript.

APPENDIX: THE CRITICAL FREQUENCY

The complex function of CMF can be expressed as Re[CMF]+j Im[CMF]. Only its real part is required to evaluate two critical frequency functions. By setting Re[CMF]=0 and extracting the ω from Eq. (8), the higher (f_h) and the lower (f_ℓ) critical frequencies are obtained as

$$f_h = \frac{\varepsilon_o \sqrt{-AB}}{2\pi C}, \tag{A1}$$

$$f_\ell = -\frac{\varepsilon_o \sqrt{-E(F+G)}}{2\pi D}, \tag{A2}$$

where

$$A = -\varepsilon_c^2 - 2\varepsilon_c\varepsilon_s + \varepsilon_c\varepsilon_s\beta + \varepsilon_s^2\beta - \varepsilon_s^2,$$

$$B = -\sigma_c^2 + \beta\sigma_s^2 + \sigma_c\sigma_s\beta - \sigma_s^2 - 2\sigma_c\sigma_s,$$

$$C = \varepsilon_o^2 A,$$

$$D = \varepsilon_m\varepsilon_o^2 E,$$

$$E = \beta\sigma_s\sigma_c - \sigma_c^2 + \beta\sigma_s^2 - 2\sigma_c\sigma_s - \sigma_s^2,$$

$$F = 2\beta\sigma_m\sigma_c\sigma_s^2 + \sigma_c^2\sigma_s\sigma_m\beta - 2\sigma_c\sigma_s\sigma_m^2 - \sigma_c^2\sigma_s^2 - 2\sigma_c\sigma_m\sigma_s^2 - \sigma_m^2\sigma_s^2),$$

$$G = \beta(\sigma_m^2\sigma_s^2 + \sigma_c^2\sigma_s^2 + \sigma_c\sigma_s\sigma_m^2) - \sigma_c^2\sigma_m^2 - 2\sigma_s\sigma_m\sigma_c^2.$$

If $f_\ell = f_h$, Eq. (A1), then Eq. (A2) leads to $\sigma_{ct} = \sigma_c(2-\beta)/2(\beta-1)$, where $\beta = 1/(1-L_k)$. When the σ_s reaches the maximum (critical) value of σ_{ct}, the two frequencies merge at the zero DEP force. Note that the expression for σ_{ct} is a constant that solely depends on σ_c and L_k. At the critical value, $\sigma_{ct} = \sigma_c$ and $\beta = \frac{4}{3}$.

[1] R. Pethig, M. S. Talary, and R. S. Lee, IEEE Eng. Med. Biol. Mag. **22**, 43 (2003).
[2] M. S. Talary, J. P. H. Burt, J. A. Tame, and R. Pethig, J. Phys. D: Appl. Phys. **29**, 2198 (1996).
[3] M. P. Hughes, Nanotechnology **11**, 124 (2000).
[4] T. B. Jones, IEEE Eng. Med. Biol. Mag. **22**, 33 (2003).
[5] G. Fuhr, R. Hagedorn, T. Muller, W. Benecke, B. Wagner, and J. Gimsa, Stud. Biophys. **140**, 79 (1991).
[6] R. Hagedorn, G. Fuhr, T. Muller, and J. Gimsa, Electrophoresis **13**, 49 (1992).
[7] X. B. Wang, M. P. Hughes, Y. Huang, F. F. Becker, and P. R. C. Gascoyne, Biochim. Biophys. Acta **1243**, 185 (1995).
[8] L. M. Fu, G. B. Lee, Y. H. Lin, and R. J. Yang, Mechatronics **9**, 377 (2004).
[9] T. L. Mahaworasilpa, H. G. L. Coster, and E. P. George, Biochim. Biophys. Acta **1193**, 118 (1994).
[10] T. L. Mahaworasilpa, H. G. L. Coster, and E. P. George, Biochim. Biophys. Acta **1281**, 5 (1996).
[11] J. Gimsa and D. Wachner, Biophys. J. **75**, 1107 (1998).
[12] S. Bunthawin and P. Wanichapichart, Proceedings of the Second IEEE International Conference on Nano/Micro Engineering and Molecular Systems, 2007 (unpublished), pp. 472–477.
[13] H. A. Pohl, *Dielectrophoresis: The Behavior of Neutral Matter in Non-Uniform Electric Fields* (Cambridge University Press, Cambridge, England, 1978).
[14] K. Asami, T. Hanai, and N. Koizumi, Jpn. J. Appl. Phys., Part 1 **19**, 359 (1980).
[15] L. D. Landau and E. M. Liftschitz, *Elektrodanamik der Kontinua* (Akademie, Berlin, 1985).
[16] J. Happel and H. Brenner, *Low Reynolds Number Hydrodynamics* (Martinus Nijhoff, Boston, 1983).
[17] V. Raicu, C. Gusbeth, D. F. Anghel, and G. Turcu, Biochim. Biophys. Acta **1379**, 7 (1998).
[18] P. Wanichapichart, T. Wongluksanapan, and L. Khooburat, The Second IEEE International Conference on Nano/Micro Engineering and Molecular Systems, 2007 (unpublished), pp. 1115–1120.
[19] X. F. Zhou, G. H. Markx, and R. Pethig, Biochim. Biophys. Acta **1281**, 60 (1996).
[20] R. Pethig and G. H. Markx, "Applications of dielectrophoresis in biotechnology," TIBTECH October, Vol. 15 (reviews), pp. 426–432, 1997.